



HAL
open science

Reprogramming of Adult Retinal Müller Glial Cells into Human-Induced Pluripotent Stem Cells as an Efficient Source of Retinal Cells

Amélie Slembrouck-Brec, Amélie Rodrigues, Oriane Rabesandratana, Giuliana Gagliardi, Céline Nanteau, Stéphane Fouquet, Gilles Thuret, Sacha Reichman, Gael Orioux, Olivier Goureau

► To cite this version:

Amélie Slembrouck-Brec, Amélie Rodrigues, Oriane Rabesandratana, Giuliana Gagliardi, Céline Nanteau, et al.. Reprogramming of Adult Retinal Müller Glial Cells into Human-Induced Pluripotent Stem Cells as an Efficient Source of Retinal Cells. *Stem Cells International*, 2019, 2019, pp.7858796. 10.1155/2019/7858796 . hal-02485661

HAL Id: hal-02485661

<https://hal.sorbonne-universite.fr/hal-02485661>

Submitted on 20 Feb 2020

HAL is a multi-disciplinary open access archive for the deposit and dissemination of scientific research documents, whether they are published or not. The documents may come from teaching and research institutions in France or abroad, or from public or private research centers.

L'archive ouverte pluridisciplinaire **HAL**, est destinée au dépôt et à la diffusion de documents scientifiques de niveau recherche, publiés ou non, émanant des établissements d'enseignement et de recherche français ou étrangers, des laboratoires publics ou privés.

Reprogramming of adult retinal Müller glial cells into human induced pluripotent stem cells as an efficient source of retinal cells

Amélie Slembrouck-Brec^{1*}, Amélie Rodrigues^{1*}, Oriane Rabesandratana¹, Giuliana Gagliardi¹, Céline Nanteau¹, Stéphane Fouquet¹, Gilles Thuret², Sacha Reichman¹, Gael Orioux¹ and Olivier Goureau¹

¹ Sorbonne Université, INSERM, CNRS, Institut de la Vision, F-75012 Paris, France

² Biologie, Ingénierie et Imagerie de la Greffe de Cornée, EA2521, Faculté de Médecine, Université Jean Monnet, Saint-Etienne, France.

Correspondence should be addressed to: Olivier Goureau; olivier.goureau@inserm.fr

* These authors contributed equally to this work

Abstract

The reprogramming of human somatic cells to induced pluripotent stem cells (iPSCs) has broad applications in regenerative medicine. The generation of self-organized retinal structures from these iPSCs offers the opportunity to study retinal development and model specific retinal disease with patient-specific iPSCs, and provides the basis for cell replacement strategies. In this study we demonstrated that the major type of glial cells of the human retina, Müller cells, can be reprogrammed into iPSCs that acquire classical signature of pluripotent stem cells. These Müller glial cell-derived iPSCs were able to differentiate toward retinal fate and generate concomitantly retinal pigmented epithelial cells and self-forming retinal organoids structures containing retinal progenitor cells. Retinal organoids recapitulated retinal neurogenesis with differentiation of retinal progenitor cells into all retinal cell types in a sequential overlapping order. With a modified retinal maturation protocol characterized by the presence of serum and high glucose levels, our study revealed that the retinal organoids contained pseudo-laminated neural retina with important features reminiscent of mature photoreceptors, both rod and cone subtypes. This advanced maturation of photoreceptors supports the possibility to use 3D retinal organoids for studying photoreceptor development, but also offers novel opportunity for disease modeling, particularly for inherited retinal diseases.

1. Introduction

Human pluripotent stem cells (PSCs) represent a valuable tool to study human neuronal development and neurodegenerative diseases and to develop future stem-cell based therapies [1]. As concerns the retina, both human embryonic stem cells (ESCs) and induced pluripotent stem cells (iPSCs) have been shown to be able to produce retinal cells [2–7], including retinal ganglion cells, photoreceptors and retinal pigmented epithelial (RPE) cells, corresponding to the major cell types affected in the most common retinal degenerative diseases. The differentiation of human PSCs toward the retinal lineage has evolved considerably in the last few years and several innovative protocols allowing the self-formation of 3D retinal organoids have been reported [8–16].

Many types of somatic cells, such as skin fibroblasts, blood cells, keratinocytes or urine-derived cells, have been successfully used for reprogramming and the production of human iPSCs [1,17]. Due to their high availability through noninvasive and routine sampling in clinical settings, blood and urine-derived cells have been considered as a preferred source for reprogramming. Nevertheless, independently of the initial somatic identity of reprogrammed cells, human iPSCs can be guided to differentiate into retinal organoids with relatively similar efficiency using different retinal differentiation protocols [11,18–21]. Recently, Wang et al. reprogrammed four different neuronal cell types (rod photoreceptors, cone photoreceptors, bipolar cells and amacrine/horizontal cells) from early and late post-natal mouse retina into iPSCs and further differentiated them into retinal organoids [22]. Mouse Müller glial cells (MGCs), which originate from the same pool of retinal progenitors as retinal neurons, can also be reprogrammed to pluripotency with high efficiency and can be guided to differentiate into retinal organoids [22]. Even though no data regarding the reprogramming of human retinal cells has been reported, human glial cells such as astrocytes isolated from cerebellar tissue can be efficiently reprogrammed into iPSCs and further differentiated into different neural cell types [23,24].

Here, we report the generation of iPSCs from human MGCs. By applying our multistep retinal differentiation protocol [19], we differentiated human MGC-derived iPSCs into pseudo-laminated retinal organoids that contained all major retinal cell types.

2. Materials and Methods

2.1 Human postmortem tissue and Müller glial cell cultures

Postmortem eye tissues were collected within 24h after death from bodies donated to science (Laboratory of Anatomy, Faculty of Medicine of St-Etienne, France) in accordance with the French bioethics law. Handling of donor tissues adhered to the tenets of the Declaration of Helsinki of 1975 and its 1983 revision in protecting donor confidentiality.

Retina was dissected from globes by circumferential hemisection behind the ora serrata to gently remove the anterior segment including lens. The retina was carefully separated from the vitreous by transection of the papillary head and around the peripheral regions and transferred into CO₂-independent medium (Thermo Fisher Scientific). After removing the major blood vessels, the retina was chopped into small fragments (<2mm²) and cells dissociated as previously described [25,26] with some modifications. After 3 washes in Ringer solution (NaCl 155 mM; KCl 5 mM; CaCl₂ 2 mM; MgCl₂ 1 mM; NaH₂PO₄ 2 mM; HEPES 10 mM and Glucose 10 mM), retinal fragments were dissociated with pre-activated papain at 31.8 U/mg (Worthington) in Ringer solution during 30 min at 37°C. Digestion was arrested by the addition of 1 ml of DMEM (Thermo Fisher Scientific) containing 10% of fetal bovine serum (FBS) (Thermo Fisher Scientific) and 25µg/ml of DNase1 (Sigma-Aldrich). The cells were homogeneously suspended with gentle up and down pipetting in pre-warmed DMEM with 10% FBS and 10 µg/ml gentamycin (MGC-medium) and seeded in 6-cm dishes previously coated with Poly-D-Lysin at 2 µg/cm² and Laminin at 1 µg/cm² (Sigma-Aldrich). Dissociated cells were incubated at 37°C in a standard 5% CO₂ / 95% air incubator and medium was left unchanged for 3 to 5 days and then renewed every 2 to 3 days. By the end of the first week in culture, large flattened glial cells were observed with few neuron-like cells scattered on the glial surface. Mitotic glial cells became confluent within 10 to 14 days after

plating. At this time cells were passaged by a brief incubation in TrypLE Express (Thermo Fisher Scientific) and banked (cryopreservation in FBS-10%DMSO) or seeded in 6 well-plates previously coated with Poly-D-Lysin and Laminin for reprogramming.

2.2 Human Müller glial cell reprogramming and validation

Human MGCs at passage 1 were transduced using the CytoTune Sendai reprogramming vectors Oct4, Klf4, Sox2 and c-Myc (Thermo Fisher Scientific) and cultured for 6 days in MGC-medium before plating on mitomycin human foreskin (MHF)-seeded dishes. The day after, the MGC-medium was replaced with the iPS medium, corresponding to ReproStem medium (ReproCELL, Ozyme) supplemented with 10 ng/ml of human recombinant FGF2 (PreproTech France). The emergent human iPSC colonies were picked under a stereomicroscope according to their human ESC-like colony morphology and expanded on MHF feeder layers. After generation of a frozen stock, human iPSCs were cultured on MHF feeder layers and subsequently adapted to feeder-free conditions on truncated recombinant human vitronectin-coated dishes with Essential 8™ medium (both from Thermo Fisher Scientific) as previously described [19]. Cells were routinely cultured at 37°C in a standard 5% CO₂ / 95% air incubator with a daily medium change and passaged with the enzyme-free Gentle cell dissociation reagent (Thermo Fisher Scientific) every week. The undifferentiated state of iPSC colonies was characterized by alkaline phosphatase expression as previously described [11]. Between twelve and sixteen passages, the clearance of the exogenous reprogramming factors and Sendai virus genome was confirmed by qPCR following the manufacturer's instructions (Thermo Fisher Scientific). At the same time, conventional cytogenetic analysis and *in vivo* pluripotency analysis by teratoma formation assay were performed as described previously [11]. The genomic integrity was confirmed by SNP genotyping (Integrigen Genomics).

2.3 Retinal differentiation and human iPSC-derived retinal cell cultures

Retinal cell differentiation was based on our previously established protocol with adherent human iPSC [11,27]. iPSCs derived from human MGCs cultured in Essential 8™ medium were switched in chemical defined Essential 6™ medium (Thermo Fisher Scientific). After 2 days, iPSCs were cultured in E6N2 medium composed of Essential 6™ medium, 1% N2 supplement (Thermo Fisher Scientific), 10 units/ml Penicillin and 10 µg/ml Streptomycin (Thermo Fisher Scientific). The medium was changed every 2-3 days. Around Day 28 (D28), identified self-formed retinal organoids were isolated, using a needle, with the surrounding cells and cultured as floating structures in the ProB27 medium supplemented with 10 ng/ml of recombinant human FGF2 (Peprotech) and half of the medium was changed every 2-3 days. ProB27 medium is composed of chemical defined DMEM:Nutrient Mixture F-12 (DMEM/F12, 1:1, L-Glutamine), 1% MEM non-essential amino acids, 2% B27 supplement (Thermo Fisher Scientific), 10 units/ml Penicillin and 10 µg/ml Streptomycin. At D35, retinal organoids were cultured in absence of FGF2 in ProB27 medium with 10% FBS and 2mM of Glutamax for the next several weeks. To evaluate maturation of photoreceptors, at D84, the retinal organoids were cultured in ProB27 medium with 2% B27 supplement without vitamin A (Thermo Fisher Scientific) until D200.

For human iPSC-derived RPE cell cultures, identified pigmented patches were cut around D42 and transferred, noted as passage 0 (P0), onto plates coated with Geltrex (Thermo Fisher Scientific). Human iPSC-derived RPE cells were expanded in the ProN2 medium composed of DMEM/F12, 1% MEM non-essential amino acids, 1% N2 supplement, 10 units/ml Penicillin and 10 µg/ml Streptomycin and passaged or banked as previously described [19,27].

2.4 Cryosection

For cryosectioning, retinal organoids were fixed for 15 min in 4% paraformaldehyde (PAF) at 4°C and washed in Phosphate-buffered saline (PBS). Structures were incubated at 4°C in PBS / 30% Sucrose (Sigma-Aldrich) solution during at least 2 hrs and embedded in a

solution of PBS, 7.5% gelatin (Sigma-Aldrich), 10% sucrose and frozen in isopentane at -50°C. 10 µm-thick cryosections were collected in two perpendicular planes.

2.5 Immunostaining and imaging on retinal sections and dissociated cells

Dissociated cells were fixed with 4% PAF in PBS for 10 min before immunostaining. Sections and fixed dissociated cells were washed with PBS, nonspecific binding sites were blocked for 1 hr at room temperature with a PBS solution containing 0.2% gelatin and 0.1% Triton X-100 (blocking buffer) and then overnight at 4°C with the primary antibody (Table S1) diluted in blocking buffer. Slides were washed three times in PBS with 0.1% Tween and then incubated for 1 hr at room temperature with appropriate secondary antibodies conjugated with either Cy3, Alexa Fluor 488, 594 or 647 (Interchim) diluted at 1:600 in blocking buffer with 4',6-diamidino-2-phenylindole (DAPI) diluted at 1:1000 to counterstain nuclei. Fluorescent staining signals were captured with an Olympus FV1000 confocal microscope.

2.6 Retinal organoid immunostaining-clearing and imaging

Retinal organoids were fixed with 4% PAF in PBS for 30 to 60 min before immunostaining with a PBS solution containing 0.2% gelatin, 0.5% Triton X-100 and 0.01% thimerosal (Sigma-Aldrich) as previously described [11]. Samples were next submitted to the 3D imaging of solvent-cleared organ (3DISCO) clearing procedure [19]. 3D imaging was performed with an inverted confocal microscope (Olympus FV1200) with numerical objectives for high-resolution imaging. Images, 3D volume and movies were generated with Imaris x64 software (version 7.6.1, Bitplane) using the “snapshot” and “animation” tools.

2.7 RNA extraction and Taqman Assay

Total RNAs were extracted using Nucleospin RNA II kit (Macherey-Nagel) and cDNA synthesized using the QuantiTect reverse transcription kit (Qiagen) following manufacturer's recommendations. qPCR analysis was performed with custom TaqMan® Array 96-Well Fast

plates (Thermo Fisher Scientific) according to the manufacturer's protocol. All primers and MGB probes labeled with FAM for amplification were purchased from Thermo Fisher Scientific (Table S2). Results were normalized against 18S and quantification of gene expression was based on the DeltaCt Method in minimum three independent biological experiments.

2.8 Phagocytosis assay.

Photoreceptor outer segments (POS) phagocytosis assay was performed as previously described [19]. Briefly, four weeks after plating confluent human iPSC-derived RPE cells were challenged for 3 hrs with 1×10^6 FITC-labeled POS before detection of surface-bound and internalized FITC-POS particles. For exclusive detection of internalized particles, fluorescence of surface-bound FITC-POS was selectively quenched by incubation in 0.2% trypan blue before cell fixation in ice cold methanol. Following rehydration, cells were incubated with DAPI for nuclei counterstaining. Fluorescent signals were quantified with the Infinite M1000 Pro (Tecan). The immortalized rat RPE cell line RPE-J was used as a positive control for phagocytic activity.

3. Results

3.1 Derivation of iPSCs from human Muller cells

Retinal cells were dissociated from human postmortem retina and were seeded into tissue culture plates and left to develop as monolayer culture for one week in culture conditions previously described to favor glial cell culture while eliminating other cell types [25]. After one passage, immunostaining of the cells with anti-Vimentin and anti-Glutamine Synthase (GS) antibodies revealed homogenous labeling throughout the cytoplasm of the cells, consistent with a MGC phenotype (Figures 1A-1B). In contrast, markers of microglia and monocytes/macrophages such as Ionized calcium binding adaptor molecule 1 (Iba1) and CD18 were absent (Figures 1A-1B). We investigated the potential of human MGCs to be reprogrammed into PSCs using the four reprogramming factors OCT3/4, SOX2, CMYC and

KLF4 delivered using non-integrative Sendai viruses previously used for dermal fibroblast reprogramming [28]. Emerging iPSC colonies were detectable between 10 and 15 days after transduction and around 10 colonies were picked up and expanded for at least 5 passages before being adapted in feeder-free conditions (vitronectin coating). Expanded human iPSC colonies displayed alkaline phosphatase activity as shown in Figure 1C for one clone (iPSC line 5f). Immunofluorescence analysis of human iPSC line-5f revealed co-expression of transcription factors OCT4 and SOX2, and surface markers SSEA4 and TRA1-81 (Figures 1D-1E), characteristic of pluripotent stem cells. RT-qPCR revealed that the expression of pluripotency genes markedly increased over the respective human MGC population and was similar with that seen in human ESCs (Figure 1F).

Human iPSC line-5f could be differentiated *in vivo* into derivatives of all three germ layers, as shown by teratoma formation in NSG mouse (Figure S1A-S1B), and exhibited a normal karyotype after 15 passages (Figure S1C). The clearance of the vectors and the exogenous reprogramming factor genes was confirmed by qPCR after 15 passages (Figure S1D). Furthermore, genomic integrity of the iPSC line-5f was confirmed by SNP genotyping (Figure S1E).

3.2 Induction of human MGC-derived iPSCs towards retina cell fates

Based on our retinal differentiation protocol in xeno-free / feeder-free conditions [19,27], we first evaluated the ability of overgrowing human MGC-derived iPSCs to give rise to neuroepithelial-like structures that could acquire an eye field (EF) fate. As previously reported for iPSCs derived from dermal fibroblasts, self-forming neuroepithelial-like structures can be observed about 4 weeks after the initiation of differentiation (Figure 2A). RT-qPCR analysis demonstrated that cells of 28-day-old (D28) structures expressed EF transcription factors, such as *LHX2*, *MITF*, *PAX6*, *RAX*, *SIX3* and *VSX2*, while losing the expression of the pluripotency marker *POU5F1*, and showed low or no expression of forebrain and midbrain markers, such as *EN1* and *NKX2-1* (Figure 2B). Interestingly, the expression of transcription factors involved in the photoreceptor lineage, such as *CRX*, *NRL*,

and *NEUROD1*, was also detected (Figure 2B). In previously published 3D induction protocols, inhibition of Wnt and BMP/TGF β pathways contributed to directing human PSCs to a retinal identity [7,16]. In our protocol, RT-qPCR analysis demonstrated that differentiating human MGC-derived iPSCs expressed *DKK1* and *NOGGIN*, endogenous antagonists of Wnt and BMP respectively (Figure 2C). In these conditions, inhibition of BMP/TGF and Wnt functions could occur in absence of exogenous inhibitors, enabling the formation of neuroepithelial structures after 14 days. Activation of Insulin/Insulin-like growth factor-1 signaling pathway has been also reported to contribute to directing pluripotent stem cells toward a retinal identity [13,16]. To test the possible role of this signaling pathway, we added the pharmacological inhibitor (OSI-906) of Insulin and Insulin-like growth factor-1 receptor signaling to the E6N2 medium at day 2. In this condition, very rare neuroepithelial-like structures were observed after 28 days compared to the control conditions (Figure 2A). All these results suggested that the activation of Insulin/IGF-1 pathway and endogenous production Wnt and BMP antagonists could explain the self-formation of these structures. After mechanical detachment at D28, structures were collected for further culture in suspension in the presence of FGF2 for one week to favor differentiation of the neural retina (Figure 2D). Co-expression of RAX and PAX6 detected by immunostaining of sections from D35 organoids (after one week in floating culture), confirmed the EF identity of the organoids (Figure 2E). PAX6-positive cells located in the outer part of the developing neuroepithelium also expressed the retinal progenitor cell marker VSX2 (Figure 2F). At D35, many VSX2-positive cells were still mitotic as revealed by the Ki67 proliferation marker staining (Figure 2G), confirming the retinal progenitor cell phenotype of these cells.

3.3 Formation of retinal organoids from human MGC-derived iPSCs

During retinal development, multipotent retinal progenitors can give rise to all retinal cell types in a defined overlapping chronological order with early-born cell types like retinal ganglion cells (RGCs), horizontal/amacrine cells and late-born cell types including bipolar cells and MGCs. Regarding photoreceptors, cones are mostly produced during early stages

of retinal development, whereas rods are generated later [29,30]. To assess the identity of differentiating retinal cells within organoids, immunohistochemistry was performed on sections after different periods in floating culture conditions, based on our previous retinal differentiation protocol (see methods 2.3 for details). At D56, BRN3A-positive RGCs were scattered throughout the organoid with a higher concentration at the inner-most part of the forming neural retina (Figure 3A), while cells committed toward photoreceptor lineage expressing CRX and Recoverin (RCVRN) were found on the opposite side of the structure, in the external part of the retinal organoids (Figure 3A-C). Sparse horizontal cells expressing transcription factor LHX1 can also be detected at the same time (Figure 3B). Immunostaining of D56 retinal organoid sections with the exclusive markers CRX for photoreceptors and PAX6 for early-born non-photoreceptor cells (RGCs, amacrine/horizontal cells) showed that PAX6-positive neurons and CRX-positive photoreceptors started to form two distinct layers (Figure 3C). Interestingly, cells displaying the highest level of PAX6 were found in the most central part of the structure, while in the external part of the retinal organoid, Pax6-positive cells displayed low level of expression of this transcription factor. As time progressed, these two layers can be more distinctly visualized, as shown by the exclusive location of CRX-expressing photoreceptors and PAX6-positive cells at D100 (Figure 3D) and D150 (Figure 3G). In addition to displaying a pseudo lamination with both presumptive outer nuclear layer (ONL) and inner nuclear layer (INL), retinal organoids also showed organized PAX6-positive neurons presented towards the basal surface, where RGCs are located, and also localized in the presumptive INL (Figure 3D-E). Amacrine cells identified by PAX6 and AP-2 co-staining formed a clear nuclear layer at D100, while sparsely distributed PAX6-positive / AP-2-negative cells in the apical part of the presumptive INL could correspond to the horizontal cells (Figure 3E). The population of CRX/Recoverin-positive photoreceptors congregated at the outer part of the retinal organoids (Figure 3F), corresponding to the presumptive ONL. Consistent with *in vivo* retinogenesis, late-born bipolar cells can be identified by co-staining with PKC α and VSX2 antibodies (Figure 3H), demonstrating that our culture conditions allowed the generation of all five types of retinal neurons in organoids. Furthermore, RPCs

were also able to differentiate in MGCs, as shown by the presence of cells co-expressing Glutamine Synthase (GS) and the transcription factor SOX9 in D175 retinal organoids (Figure 3I).

When retinal organoids from human MGC-derived iPSCs were subjected to differentiation in ProB27 medium in absence of FBS and Glutamax, efficient retinal differentiation was still observed with the presence of RGCs expressing BRN3A in D56 organoids and photoreceptors identified by Recoverin and CRX immunostaining in D56 and D100 organoids (Figure 4). However, organoids failed to display a continuous laminar organization with the neuro-epithelial layer mostly developing into small rosettes, where the innermost cells expressed photoreceptor markers, surrounded by PAX6-positive non-photoreceptor cells (Figure 4). This phenotype was similar to previously characterized iPSC line (hiPSC-2 clone) derived from human fibroblasts [19]. Interestingly, pseudo-laminated retinal organoids can also be obtained from this hiPSC-2 line in presence of 10%FBS and Glutamax, with similar formation of presumptive ONL, bearing CRX and Recoverin-positive photoreceptors, and presumptive INL containing PAX6-positive cells, including amacrine cells expressing AP-2 (Figure S2). Cone arrestin (CAR) immunostaining was also restricted to the presumptive ONL (Figure S2), confirming that the generation of pseudo-laminated organoids was independent on the iPSC line used as a source for differentiation and was rather due to the refinement of our original retinal differentiation protocol [19,27].

3.4 Maturation of rods and cones in retinal organoids

Next, we sought to study the maturation of photoreceptor precursors, previously identified with CRX staining (Figure 3), in presence of FBS and Glutamax for long-term culture. Constant application of Retinoic Acid (RA) has been reported to inhibit cone maturation in zebrafish [31] and recently in mouse PSC-derived retinal organoids [32]. Exogenous RA was never present in our culture conditions. Retinal organoids first cultured with normal B27 supplement containing vitamin A were switched at D84 in ProB27 medium with B27 supplement without vitamin A to prevent the formation of endogenous RA, one active

metabolite of Vitamin A. Rods and cones can be clearly identified either by Rhodopsin or Cone arrestin immunostaining restricted to the apical presumptive ONL in D175 retinal organoids (Figure 5). Rhodopsin staining was distributed throughout the soma of rods and intensively stained the peripheral region of the presumptive ONL, reflecting the formation of outer segment (OS)-like structures (Figure 5B and 5C). The ciliary protein ARL13B presented an expected punctuated labeling pattern closed to the presumptive ONL, indicating the formation of correctly positioned IS and OS-like structures (Figure 5B). Both short wavelength Opsin (Blue Opsin) and long/medium wavelength Opsin (R/G Opsin) cones were observed with the presence of specific cone pedicle-like structures, apical to the presumptive ONL (Figure 5D and 5E). To visualize photoreceptors in 3D, we performed high-resolution confocal imaging of immunolabelled D175 whole organoids subjected to 3DISCO clearing procedure [19]. Spatial arrangement of cones characterized by the expression of CRX and Cone arrestin was observed on 3D-reconstructed images with unambiguous morphological stubby bud-like cone features (Figure 5F and 5G; Video S1).

3.5 Generation of RPE cells from human MGC-derived iPSCs

After removal of retinal organoids and further differentiation of iPSC cultures in proneural medium, pigmented patches of cells appeared around D42 and could be mechanically isolated and spread onto new plates for expansion and amplification. After 4 weeks, pigmented cells formed a confluent monolayer with a cobblestone-shaped morphology (Figure 6A) and expressed the RPE-specific transcription factor MITF and the tight junction marker ZO-1 (Figure 6B). Z-stack analysis of confocal images showed the expression of Ezrin at the apical side of the cells and basolateral localization of Bestrophin (Figure 6C and 6D), which is consistent with a mature polarized RPE. RT-qPCR studies demonstrated that iPSC-derived RPE cells expressed classic markers of RPE such as *PEDF*, *MERTK*, *RPE65* and *BEST1* after long-term cultures (Figure 6E). We also evaluated the functionality of the iPSC-derived RPE cells by measuring phagocytosis of fluorescent-labeled photoreceptor outer segments (POS). As shown in Figure 5F, iPSC-derived RPE cells after one passage

were able to phagocytose with an average of 37.3 ± 0.07 % (mean \pm SEM; n=3) internalized POS within 3 hours, similar to the control rat RPE-J cell line (49.6 ± 0.02 ; mean \pm SEM; n=3).

4. Discussion

In this study we generated iPSCs from a differentiated cell type isolated from normal human retina and showed that these human iPSCs derived from MGCs can be efficiently differentiated toward retinal lineage with simultaneous formation of RPE cells and retinal organoids. Specification and maturation of retinal cells generated from MGC-derived iPSCs follow the same spatial-temporal pattern observed with retinal cells derived from other human somatic-derived iPSCs and consistent with *in vivo* development.

Since all body cells seem to have the potential to become iPSCs, though at different yields, it is not surprising that glial cells from the retina, such as MGCs can be reprogrammed into iPSCs. Furthermore, MGCs represent the most plastic cell type found in the retina. In cold-blood vertebrate, MGC population constitutes an adult retinal stem cell niche able to dedifferentiate, proliferate and generate new retinal cells, mainly after activation of the *Ascl1/Lin28* pathway following injury [33,34]. This physiologic response is absent in mammals but *in vivo* ectopic expression of a specific combination of factors targeting mouse MGCs enabled MGCs to generate functional retinal neurons in different conditions [35,36], confirming the latent stem cell potential of MGCs even in mammals.

Detailed examination of a variety of iPSCs has shown that these cells can retain some epigenetic memory of the cell of origin that bias their differentiation tendency toward the original cell type [37,38]. While this phenomenon was obvious in early-passage iPSCs, the differences in epigenetics and differentiation capacities tended to be attenuated after prolonged passages [37,38]. Other studies have shown that the cell type of origin contributed minimally to iPSC variability and that the variations in differentiation were largely attributable to donor differences rather than to the original cell type [39–41]. Even though no epigenetic characterizations have been done on the iPSCs used in this study, either derived from human MGCs or from dermal fibroblasts [11,19], no major difference in the characteristics of

retinal organoids has been observed. In agreement with our observation, Capowski et al. recently reported the ability of human iPSCs derived from fibroblasts or blood cells to generate retinal organoids, demonstrating the reproducibility of retinal organoid generation independently of the starting cell type [21]. A different observation has been made using mouse iPSCs derived from different retinal cell types [42]. These authors showed that rod-derived iPSCs were more efficient to differentiate into retinal structures containing all retinal cell types compared to structures obtained from iPSCs derived from fibroblasts. The authors hypothesized that epigenetic memory and especially the methylation status of *Lhx9* gene could explain these differences. Epigenetic differences could be lower between human fibroblasts and human MGCs than between mouse fibroblasts and mouse photoreceptors. However, retinal organoids generated from mouse ESCs or iPSCs by other groups with relatively similar protocols of differentiation never reported a significant impact of the source of cells on the formation of retinal organoids [43–46].

The number of methods for generating 3D retinal cultures from human PSCs has greatly increased in the past five years [11–16,18–21], all seeking at reproducing, despite few differences, the key steps of retinal development that are highly conserved throughout the vertebrate evolution. Morphological, cellular and molecular analysis allow to determine the identity and the distribution of retinal cell types at different stages of organoid formation. As in many 3D protocols of differentiation, we can distinguish three successive stages in cultures of differentiating organoids. Early organoids around D35 correspond essentially to expansion of RPCs within the neuroepithelial cell layer. At intermediate stages (between D50-D100), a clear separation between presumptive ONL and INL -corresponding to differentiation of photoreceptors and neuron populations of inner retina- could be observed in the majority of organoids. Finally, in late retinal organoids (D150-D175), an advanced stage of photoreceptor development can be obtained, revealed by the formation of IS and OS, within an expected time range regarding human development during which OS formed and elongated between fetal weeks 23 and 30 [47,48]. However, a progressive disorganization of the inner region of the structures was observed concurrently with the RGC loss that is

expected in this type of cultures in absence of central projections targets. The requirement of RGCs for proper retinal lamination has been demonstrated in mouse and zebrafish retina, where the developmental ablation of a RGC subpopulation or interfering with the RGC migration and positioning led to a lamination defect [49,50]. Neuronal migration and lamination play central role in the building of the retinal laminar architecture [51]. It is likely that human iPSC-derived retinal organoids do not entirely recapitulate this highly controlled process of neuronal layering that takes place during retinogenesis. It is also important to consider that *in vivo* the inner retina is vascularized in contrast to the outer retina; thus, the absence of vasculature in retinal organoids could limit the metabolic support of the inner retina structures and explain the disorganization for long-term culture. Absence of RPE could also contribute to impaired organoid lamination. Even though our protocol allowed the generation of RPE cells from iPSCs, this monolayer of epithelial cells facing the photoreceptors *in vivo* is not present in retinal organoids as a monolayer. As reported in mice, ablation of RPE during early retinal development is accompanied by disruption of retinal lamination with formation of rosette [52].

In this study we used FBS and Glutamax for long-term maintenance of cell survival [18] without addition of RA to the media throughout the whole differentiation process in order to try optimizing cone differentiation. Indeed, RA signaling pathway plays an important role in photoreceptor development by promoting rod differentiation but inhibiting cone maturation in chicken and zebrafish [31,53–55]. Recently, different groups reported that continued supplementation of RA hindered or prevented the expression of cone markers in retinal organoids derived from mouse or human iPSCs [18,32] and that exogenous RA addition was not required to generate retinal organoids with both mature rod and cone photoreceptors [20]. Most of the recent protocols aiming at generating retinal organoids applied a relatively high concentration of RA in the culture medium in a specific time window, generally before photoreceptor maturation (around day 85-120 depending of the protocol used, yielding rod-enriched organoids [14,15,21]. In our culture conditions, the precursor of RA, Vitamin A, is present in B27 supplement only at early time of organoid floating cultures but not for long-

term cultures (after 12 weeks), in attempt to control the endogenous RA production during the culture. It would be interesting to investigate the expression of RA-synthesizing enzymes (Aldh1a1 and Aldh1a3) and catabolizing enzymes (Cyp26a1 and Cyp26a3) in human retinal organoids at different stages of maturation, since the transient and highly localized expression pattern of these enzymes in human fetal retina could explain the foveal patterning [55]. Recent data in mouse PSC-derived retinal organoids reported a drastic down-regulation of RA metabolism enzymes (Raldh1, Raldh3 and Cyp26a1) at late differentiation stages, when cone precursors are present [32]. As reported by other groups [18,20,21,56], we found that human organoids have similar distribution of cone subtypes, with less blue cones than red/green cones, as to the *in vivo* situation of human retina. The control of cone subtype specification by thyroid hormone signaling, largely described in mice [29,30], was recently confirmed in human PSC-derived retinal organoids by elegant CRISPR/Cas9-mediated gene editing [56]. In our study, the presence of triiodothyronine (T3), the most active form of thyroid hormone in the B27 supplement, makes possible to control the cone subtype specification in retinal organoids via the thyroid hormone receptor beta.

In summary, stem cell-derived retinal organoid technology represents a useful tool for studying the development of human retina and for modeling human retinal diseases, particularly those targeting the outer retina. With the generation of relevant cells, this innovative technology is expected to facilitate the development of cell therapies for retinal dystrophies.

5. Data Availability

The data used to support the findings of this study are available from the corresponding author upon request.

6. Conflicts of interest

The authors declare that they have no conflicts of interest.

7. Author's Contributions

A.S-B. conception and design, collection and/or assembly of data, data analysis and interpretation and revision of manuscript. A.R conception and design, collection and/or assembly of data, data analysis and interpretation and revision of manuscript. O.R collection and/or assembly of data and revision of manuscript. G.G. collection and/or assembly of data and revision of manuscript. C.N. collection and/or assembly of data. S.F. collection and/or assembly of data. G.T. provision of study material. S.R. data analysis and interpretation. G.O collection and/or assembly of data, data analysis and interpretation, manuscript writing. O.G. conception and design, data analysis and interpretation, manuscript writing and financial support.

8. Funding statement

This work was supported by grants from the “Agence Nationale de la Recherche” (ANR-15-RHUS-001; ANR-16-CE17-0008-02 and ANR-17-CE18-0004-01), the LABEX Revive [ANR-10-LABX-73], the LABEX LifeSenses [ANR-10-LABX-65], the Technology Transfer company SATT Lutec and Retina France association. O.R. was a recipient of a PhD fellowship from Fédération des Aveugles de France and G.G. a recipient of a PhD fellowship from the French Ministry of Higher Education and Research.

9. Acknowledgments

The authors would like to thank Professor José-Alain Sahel (Director of the “Institut de la Vision”) for administrative and financial support and K. Marazova for comments and advice on the manuscript. We thank V. Fradot for valuable advice in Müller glial cell cultures, N. Oudrhiri and A. Bennaceur, (GHU Paris-Sud APHP) for the conventional cytogenetic analysis and Dr. C. Craft (Mary D. Allen Laboratory for Vision Research, USC ROSKI Eye Institute) for Cone arrestin antibody.

10. Supplementary Material

Figure S1: Additional characterization of human MGC-derived iPSC lines

Figure S2: Reproducibility of retinal organoid lamination and photoreceptor differentiation with a human iPSC line derived from fibroblasts.

Table S1: List of antibodies used for immunohistochemistry analysis

Table S2: List of TaqMan® Gene Expression ID Assays used for RT-qPCR

Movie S1: Movie of a D175 retinal organoid labelled with anti-CRX (white) and Cone arrestin (red). Scale bar = 300µm.

11. References

- 1 Karagiannis P, Takahashi K, Saito M, et al. Induced Pluripotent Stem Cells and Their Use in Human Models of Disease and Development. *Physiol Rev* 2019; 99:79–114.
- 2 Wiley LA, Burnight ER, Songstad AE, et al. Patient-specific induced pluripotent stem cells (iPSCs) for the study and treatment of retinal degenerative diseases. *Prog Retin Eye Res* 2015; 44:15–35.
- 3 Leach LL, Clegg DO. Concise Review: Making Stem Cells Retinal: Methods for Deriving Retinal Pigment Epithelium and Implications for Patients With Ocular Disease. *Stem Cells* 2015; 33:2363–2373.
- 4 Zhao C, Wang Q, Temple S. Stem cell therapies for retinal diseases: recapitulating development to replace degenerated cells. *Development* 2017; 144:1368–1381.
- 5 Rabesandratana O, Goureau O, Orioux G. Pluripotent Stem Cell-Based Approaches to Explore and Treat Optic Neuropathies. *Front Neurosci* 2018; 12:651.
- 6 Jin Z-B, Gao M-L, Deng W-L, et al. Stemming retinal regeneration with pluripotent stem cells. *Prog Retin Eye Res* 2018; Nov 2018 (doi: 10.1016/j.preteyeres.2018.11.003).
- 7 Gagliardi G, Ben M'Barek K, Goureau O. Photoreceptor cell replacement in macular degeneration and retinitis pigmentosa: A pluripotent stem cell-based approach. *Prog Retin Eye Res* 2019; Mar 16 (doi: 10.1016/j.preteyeres.2019.03.001).
- 8 Meyer JS, Howden SE, Wallace KA, et al. Optic Vesicle-like Structures Derived from Human Pluripotent Stem Cells Facilitate a Customized Approach to Retinal Disease Treatment. *Stem Cells* 2011; 29:1206–1218.
- 9 Nakano T, Ando S, Takata N, et al. Self-Formation of Optic Cups and Storable

- Stratified Neural Retina from Human ESCs. *Cell Stem Cell* 2012; 10:771–785.
- 10 Tucker BA, Mullins RF, Streb LM, et al. Patient-specific iPSC-derived photoreceptor precursor cells as a means to investigate retinitis pigmentosa. *Elife* 2013; 2:e00824.
 - 11 Reichman S, Terray A, Slembrouck A, et al. From confluent human iPS cells to self-forming neural retina and retinal pigmented epithelium. *Proc Natl Acad Sci* 2014; 111:8518–8523.
 - 12 Kuwahara A, Ozone C, Nakano T, et al. Generation of a ciliary margin-like stem cell niche from self-organizing human retinal tissue. *Nat Commun* 2015; 6:6286.
 - 13 Mellough CB, Collin J, Khazim M, et al. IGF-1 Signaling Plays an Important Role in the Formation of Three-Dimensional Laminated Neural Retina and Other Ocular Structures From Human Embryonic Stem Cells. *Stem Cells* 2015; 33:2416–2430.
 - 14 Wahlin KJ, Maruotti JA, Sripathi SR, et al. Photoreceptor Outer Segment-like Structures in Long-Term 3D Retinas from Human Pluripotent Stem Cells. *Sci Rep* 2017; 7:766.
 - 15 Gonzalez-Cordero A, Kruczek K, Naeem A, et al. Recapitulation of Human Retinal Development from Human Pluripotent Stem Cells Generates Transplantable Populations of Cone Photoreceptors. *Stem Cell Reports* 2017; 9:820–837.
 - 16 Llonch S, Carido M, Ader M. Organoid technology for retinal repair. *Dev Biol* 2018; 433:132–143.
 - 17 González F, Boué S, Belmonte JCI. Methods for making induced pluripotent stem cells: reprogramming à la carte. *Nat Rev Genet* 2011; 12:231–242.
 - 18 Zhong X, Gutierrez C, Xue T, et al. Generation of three-dimensional retinal tissue with functional photoreceptors from human iPSCs. *Nat Commun* 2014; 5:4047.
 - 19 Reichman S, Slembrouck A, Gagliardi G, et al. Generation of Storable Retinal Organoids and Retinal Pigmented Epithelium from Adherent Human iPS Cells in Xeno-Free and Feeder-Free Conditions. *Stem Cells* 2017; 35:1176–1188.
 - 20 Li G, Xie B, He L, et al. Generation of Retinal Organoids with Mature Rods and Cones from Urine-Derived Human Induced Pluripotent Stem Cells. *Stem Cells Int* 2018; 2018:1–12.
 - 21 Capowski EE, Samimi K, Mayerl SJ, et al. Reproducibility and staging of 3D human retinal organoids across multiple pluripotent stem cell lines. *Development* 2019; 146:dev171686.
 - 22 Wang L, Hiler D, Xu B, et al. Retinal Cell Type DNA Methylation and Histone Modifications Predict Reprogramming Efficiency and Retinogenesis in 3D Organoid Cultures. *Cell Rep* 2018; 22:2601–2614.
 - 23 Ruiz S, Brennand K, Panopoulos AD, et al. High-Efficient Generation of Induced Pluripotent Stem Cells from Human Astrocytes. *PLoS One* 2010; 5:e15526.

- 24 Tian C, Wang Y, Sun L, et al. Reprogrammed mouse astrocytes retain a “memory” of tissue origin and possess more tendencies for neuronal differentiation than reprogrammed mouse embryonic fibroblasts. *Protein Cell* 2011; 2:128–140.
- 25 Hicks D, Courtois Y. The growth and behaviour of rat retinal Müller cells in vitro. 1. An improved method for isolation and culture. *Exp Eye Res* 1990; 51:119–129.
- 26 Gaudin C, Forster V, Sahel J, et al. Survival and regeneration of adult human and other mammalian photoreceptors in culture. *Investig Ophthalmol Vis Sci* 1996; 37:2258–2268.
- 27 Slembrouck-Brec A, Nanteau C, Sahel J-A, et al. Defined Xeno-free and Feeder-free Culture Conditions for the Generation of Human iPSC-derived Retinal Cell Models. *J Vis Exp* 2018; Sep 6.
- 28 Terray A, Fort V, Slembrouck A, et al. Establishment of an induced pluripotent stem (iPS) cell line from dermal fibroblasts of an asymptomatic patient with dominant PRPF31 mutation. *Stem Cell Res* 2017; 25:26–29.
- 29 Brzezinski JA, Reh TA. Photoreceptor cell fate specification in vertebrates. *Development* 2015; 142:3263–3273.
- 30 Wang S, Cepko CL. Photoreceptor Fate Determination in the Vertebrate Retina. *Investig Ophthalmol Vis Sci* 2016; 57:ORSFe1.
- 31 Stevens CB, Cameron DA, Stenkamp DL. Plasticity of photoreceptor-generating retinal progenitors revealed by prolonged retinoic acid exposure. *BMC Dev Biol* 2011; 11:51.
- 32 Kruczek K, Gonzalez-Cordero A, Goh D, et al. Differentiation and Transplantation of Embryonic Stem Cell-Derived Cone Photoreceptors into a Mouse Model of End-Stage Retinal Degeneration. *Stem Cell Reports* 2017; 8:1659–1674.
- 33 Hamon A, Roger JE, Yang X-J, et al. Müller glial cell-dependent regeneration of the neural retina: An overview across vertebrate model systems. *Dev Dyn* 2016; 245:727–738.
- 34 Goldman D. Müller glial cell reprogramming and retina regeneration. *Nat Rev Neurosci* 2014; 15:431–442.
- 35 Jorstad NL, Wilken MS, Grimes WN, et al. Stimulation of functional neuronal regeneration from Müller glia in adult mice. *Nature* 2017; 548:103–107.
- 36 Yao K, Qiu S, Wang Y V., et al. Restoration of vision after de novo genesis of rod photoreceptors in mammalian retinas. *Nature* 2018; 560:484–488.
- 37 Polo JM, Liu S, Figueroa ME, et al. Cell type of origin influences the molecular and functional properties of mouse induced pluripotent stem cells. *Nat Biotechnol* 2010; 28:848–855.
- 38 Kim K, Zhao R, Doi A, et al. Donor cell type can influence the epigenome and

- differentiation potential of human induced pluripotent stem cells. *Nat Biotechnol* 2011; 29:1117–1119.
- 39 Kajiwara M, Aoi T, Okita K, et al. Donor-dependent variations in hepatic differentiation from human-induced pluripotent stem cells. *Proc Natl Acad Sci* 2012; 109:12538–12543.
- 40 Rouhani F, Kumasaka N, de Brito MC, et al. Genetic Background Drives Transcriptional Variation in Human Induced Pluripotent Stem Cells. *PLoS Genet* 2014; 10:e1004432.
- 41 Kyttälä A, Moraghebi R, Valensisi C, et al. Genetic Variability Overrides the Impact of Parental Cell Type and Determines iPSC Differentiation Potential. *Stem Cell Reports* 2016; 6:200–212.
- 42 Hiler D, Chen X, Hazen J, et al. Quantification of Retinogenesis in 3D Cultures Reveals Epigenetic Memory and Higher Efficiency in iPSCs Derived from Rod Photoreceptors. *Cell Stem Cell* 2015; 17:101–115.
- 43 Eiraku M, Takata N, Ishibashi H, et al. Self-organizing optic-cup morphogenesis in three-dimensional culture. *Nature* 2011; 472:51–56.
- 44 Gonzalez-Cordero A, West EL, Pearson RA, et al. Photoreceptor precursors derived from three-dimensional embryonic stem cell cultures integrate and mature within adult degenerate retina. *Nat Biotechnol* 2013; 31:741–747.
- 45 Assawachananont J, Mandai M, Okamoto S, et al. Transplantation of Embryonic and Induced Pluripotent Stem Cell-Derived 3D Retinal Sheets into Retinal Degenerative Mice. *Stem Cell Reports* 2014; 2:662–674.
- 46 Völkner M, Zschätzsch M, Rostovskaya M, et al. Retinal Organoids from Pluripotent Stem Cells Efficiently Recapitulate Retinogenesis. *Stem Cell Reports* 2016; 6:525–538.
- 47 Hendrickson A, Bumsted-O'Brien K, Natoli R, et al. Rod photoreceptor differentiation in fetal and infant human retina. *Exp Eye Res* 2008; 87:415–426.
- 48 Hoshino A, Ratnapriya R, Brooks MJ, et al. Molecular Anatomy of the Developing Human Retina. *Dev Cell* 2017;43: 763–779.e4.
- 49 Icha J, Kunath C, Rocha-Martins M, et al. Independent modes of ganglion cell translocation ensure correct lamination of the zebrafish retina. *J Cell Biol* 2016; 215:259–275.
- 50 Tufford AR, Onyak JR, Sondereker KB, et al. Melanopsin Retinal Ganglion Cells Regulate Cone Photoreceptor Lamination in the Mouse Retina. *Cell Rep* 2018; 23:2416–2428.
- 51 Amini R, Rocha-Martins M, Norden C. Neuronal Migration and Lamination in the Vertebrate Retina. *Front Neurosci* 2018; 11:742.

- 52 Raymond SM, Jackson IJ. The retinal pigmented epithelium is required for development and maintenance of the mouse neural retina. *Current Biol* 1995; 5:1286–1295.
- 53 Hyatt GA, Schmitt EA, Fadool JM, et al. Retinoic acid alters photoreceptor development in vivo. *Proc Natl Acad Sci U S A* 1996; 93:13298–13303.
- 54 Alfano G, Conte I, Caramico T, et al. Vax2 regulates retinoic acid distribution and cone opsin expression in the vertebrate eye. *Development* 2011; 138:261–271.
- 55 da Silva S, Cepko CL. Fgf8 Expression and Degradation of Retinoic Acid Are Required for Patterning a High-Acuity Area in the Retina. *Dev Cell* 2017; 42:68–81.
- 56 Eldred KC, Hadyniak SE, Hussey KA, et al. Thyroid hormone signaling specifies cone subtypes in human retinal organoids. *Science* 2018; 362(6411).

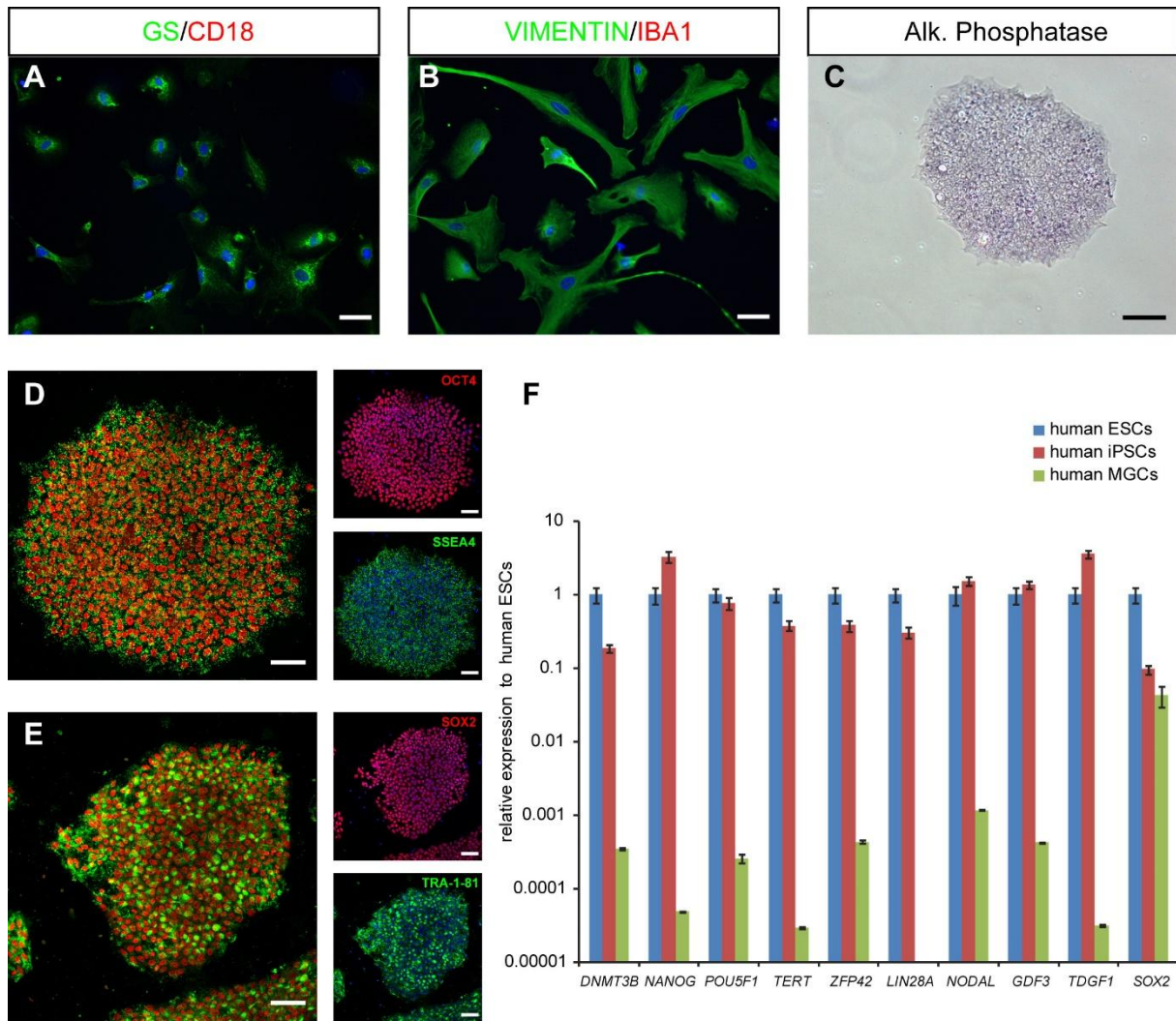


Figure 1: Derivation and characterization of iPSCs from human MGCs

(A-B) Characterization of human MGCs by immunostaining with glial (GS and Vimentin) and microglial (CD18 and Iba1) markers. Nuclei were counterstained with DAPI (blue). Note the absence of staining with microglial markers as expected. (C) Positive alkaline phosphatase staining of human iPSC-5f derived from human MGCs at P10. (D-E) Immunofluorescence of pluripotency markers (SSEA4, OCT4, TRA1-81 and SOX2) for iPSC-5f at P15. (F) qRT-PCR analysis of pluripotency and self-renewal markers in human ESCs, iPSC-5f and human MGCs. Data are normalized to human ESCs. (Scale bars: A, B, D-E, 60µm; C, 200µm).

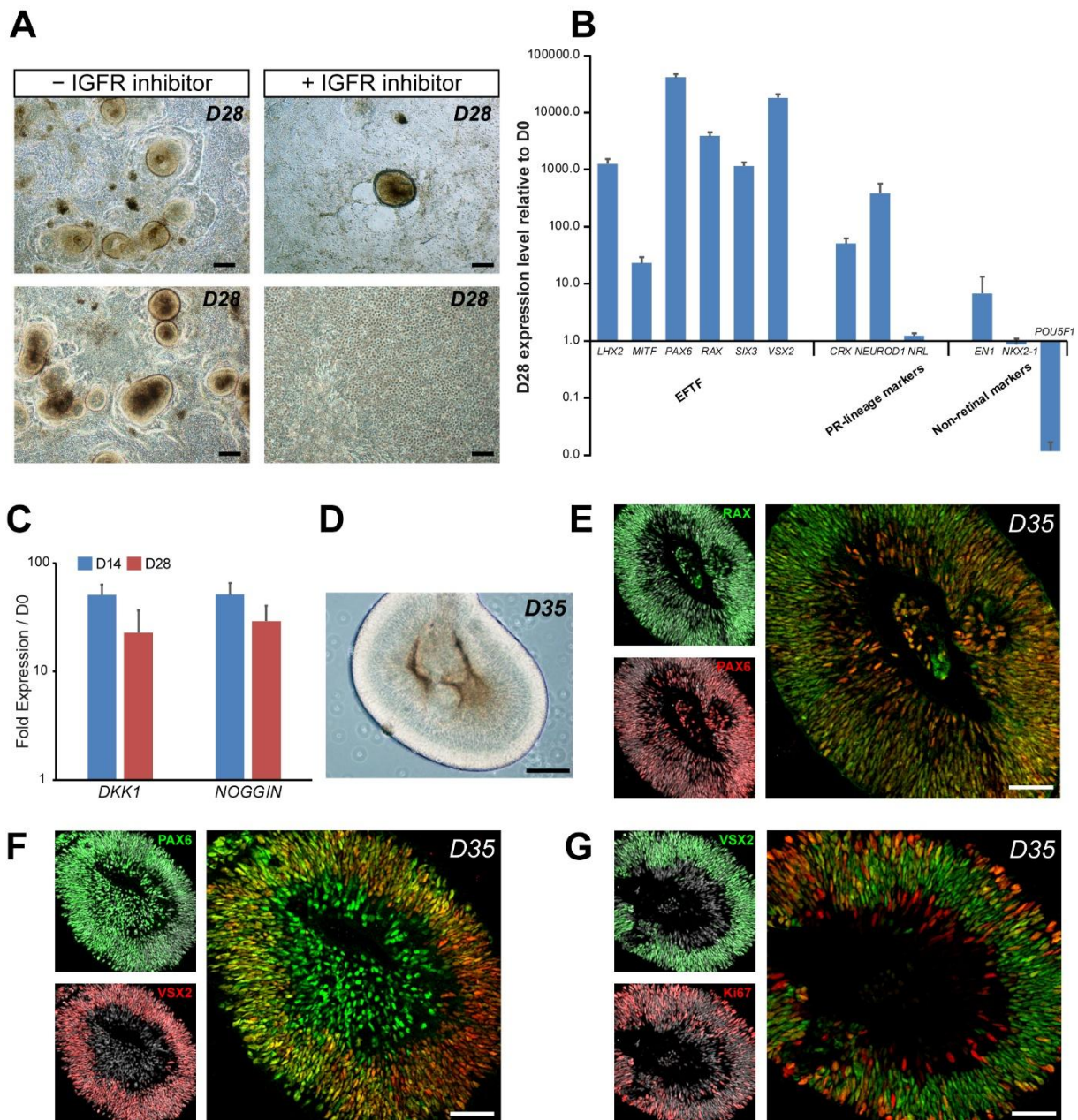


Figure 2: Commitment of human MGC-derived iPSCs into retinal lineage

(A) Examples of self-forming neuroepithelial-like structures derived from iPSC-5f at D28 and involvement of IGF-1/insulin signaling in neuroepithelium formation during iPSC differentiation. (B) qRT-PCR analysis of eye-field transcription factors (EFTF), photoreceptor-restricted lineage markers and non-retinal markers in neuroepithelial-like structures at D28. Data are normalized to iPSC-5f at D0. (C) qRT-PCR analysis of NOGGIN and DKK1 in differentiating iPSC-5f at D14 and D28. Data are normalized to iPSC-5f at D0. (E-G) Immunofluorescence co-staining of cryosections from neuroepithelial-like structures at D35 for RAX and PAX6 (E), PAX6 and VSX2 (F), or VSX2 and Ki67 (G). Nuclei were counterstained with DAPI (gray). (Scale bars: A and D, 200 μ m; E, F, G, 100 μ m).

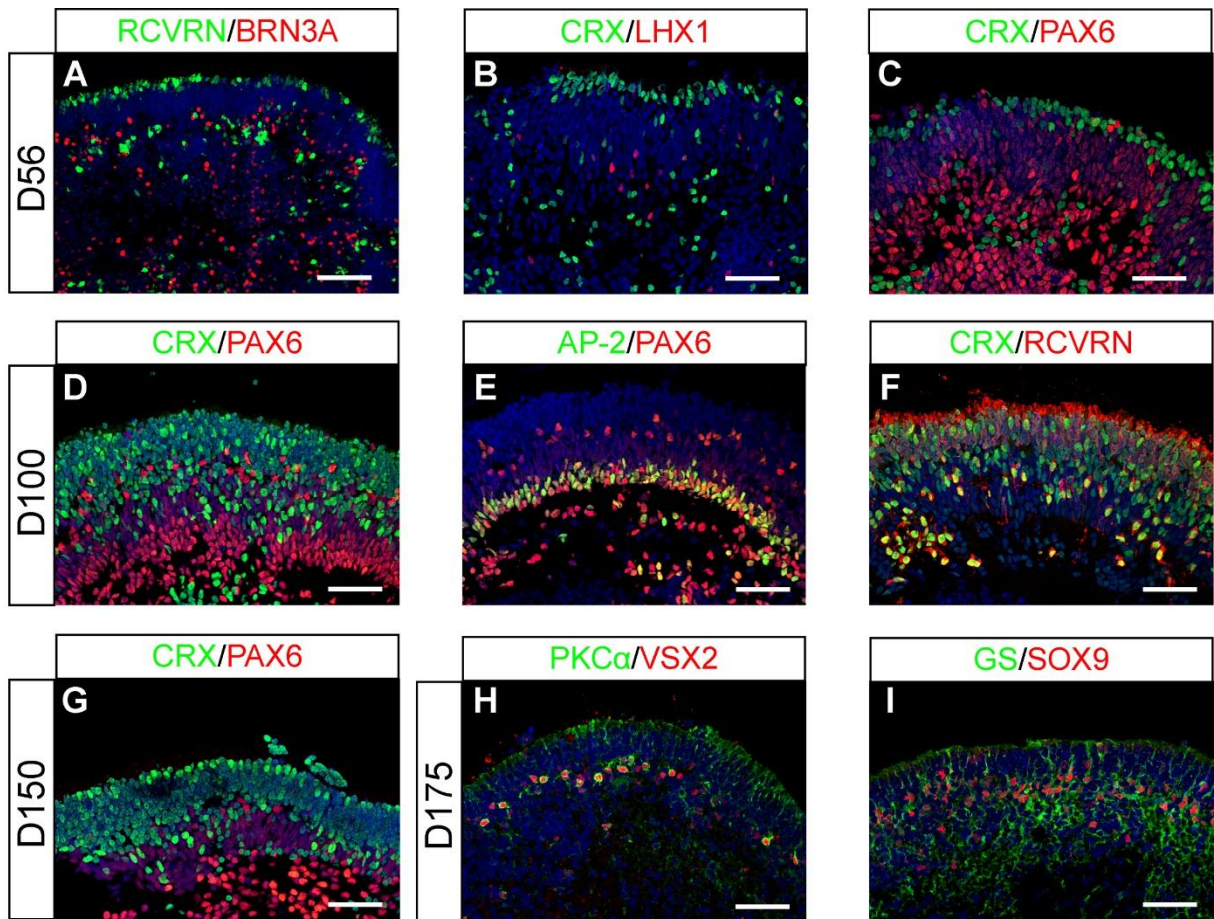


Figure 3: Generation of pseudo-laminated retinal organoids containing all retinal cell types from human MGC-derived iPSCs

(A-F) Immunofluorescence staining of cryosections from retinal organoids at D56 (A-C) and D100 (D-F) using markers for retinal ganglion cells (BRN3A, PAX6), horizontal cells (LHX1, PAX6), amacrine cells (AP2, PAX6) and photoreceptors (CRX, RCVRN).

(G-I) Immunofluorescence staining of cryosections from retinal organoids at D150 (G) and D175 (H, I) using markers for photoreceptors (CRX), bipolar cells (VSX2 and PKC α) and MGCs (GS and SOX9). Nuclei were counterstained with DAPI (blue). (Scale bars: A, 100 μ m; B-I, 50 μ m).

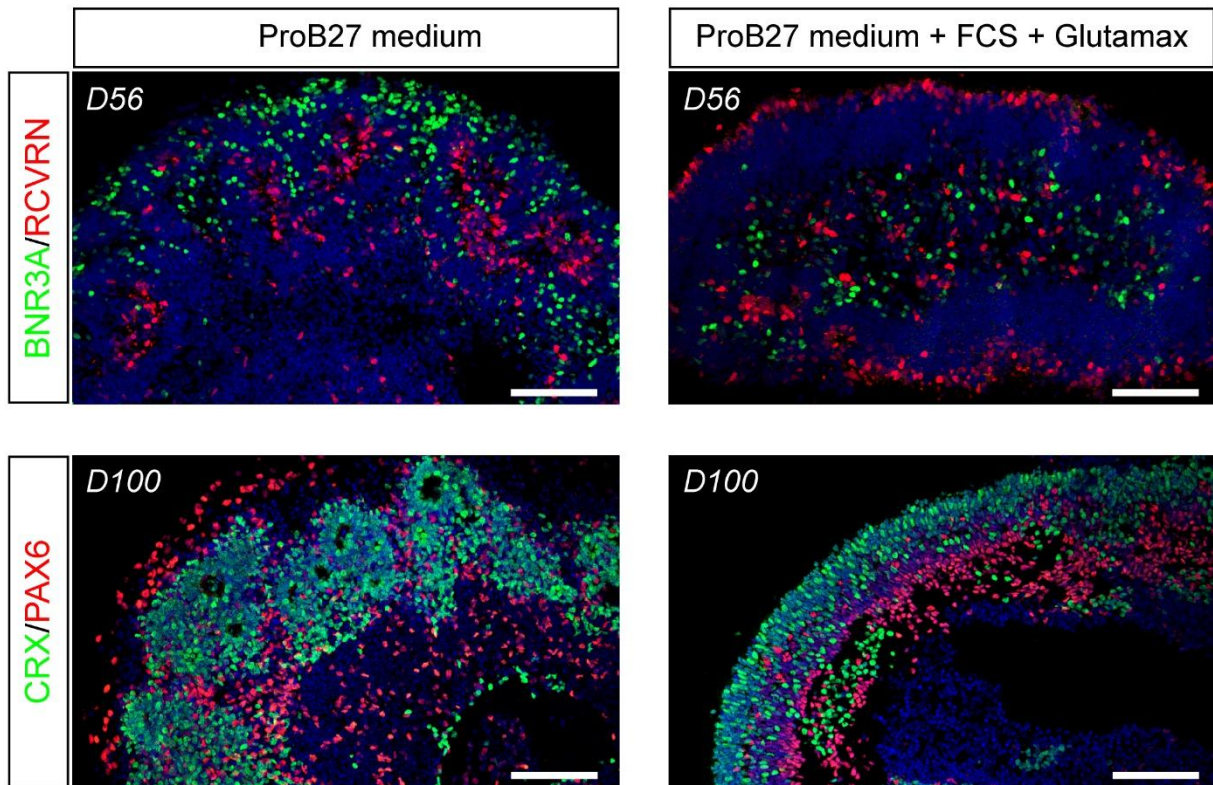


Figure 4: Improvement of retinal organoid lamination in presence of FCS and Glutamax. Immunofluorescence staining of cryosectioned retinal organoids from human MGC-derived iPSCs using markers for retinal ganglion cells (BRN3A, PAX6), amacrine/horizontal cells (PAX6) and photoreceptors (CRX) after 56 and 100 days in floating cultures in absence (left panels) or in presence (right panels) of 10%FCS and 2mM Glutamax in ProB27 medium. Nuclei were counterstained with DAPI (blue). (Scale bars: 100 μ m).

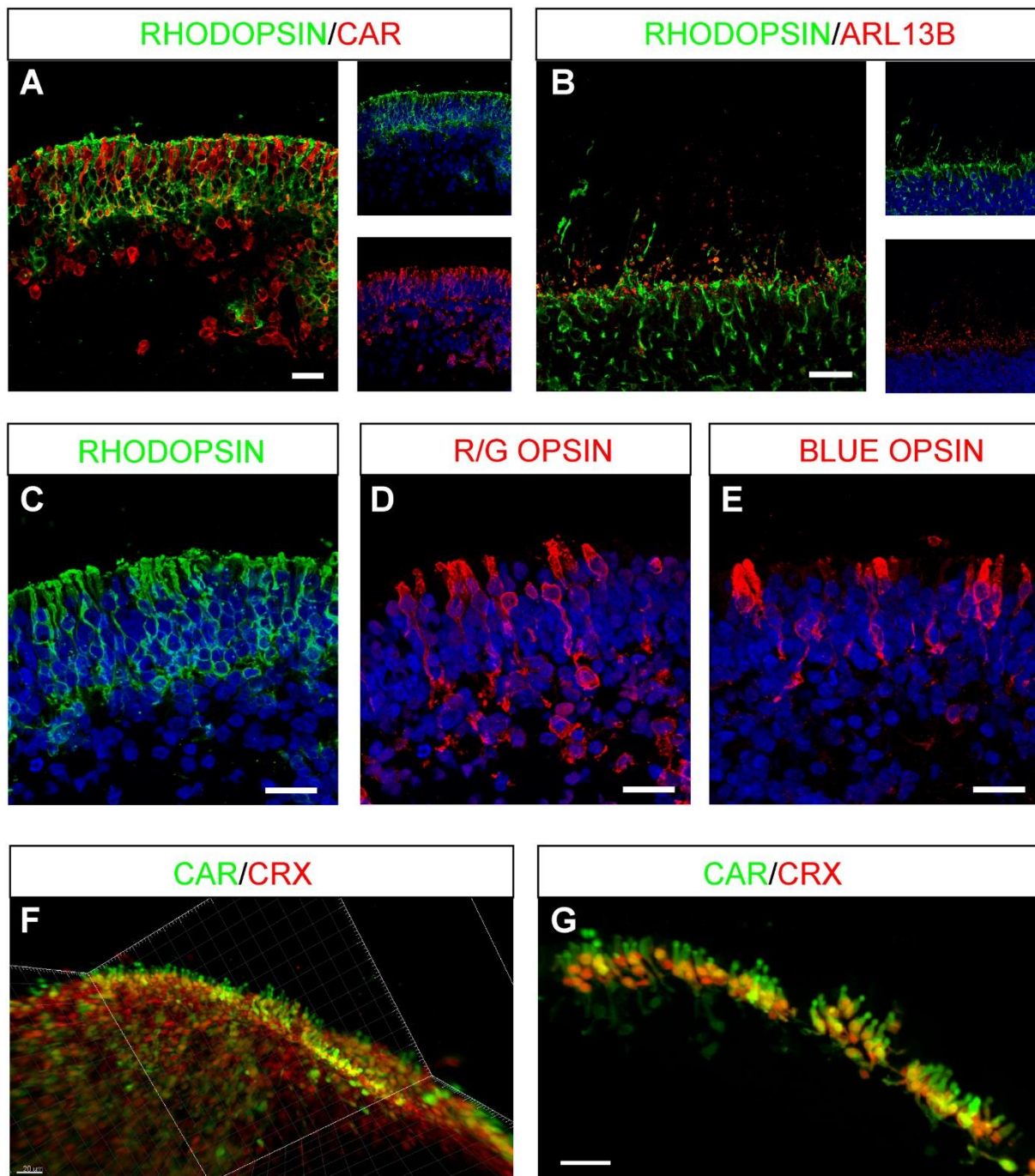


Figure 5: Photoreceptor development in retinal organoids from human MGC-derived iPSCs (A-E) Immunofluorescence staining of cryosections from retinal organoids at D175 using specific photoreceptor markers to identify both rods (RHODOPSIN), cones (CAR, R/G OPSIN, BLUE OPSIN) and cilia marker (ARL13B). Nuclei were counterstained with DAPI (blue). (F, G) 3D views of solvent-cleared D175 retinal organoids immunostained for Cone arrestin (CAR) and CRX. (G) High-magnification image of isolated cones from panel F (white frame) with Imaris software (Scale bars: 20 μ m).

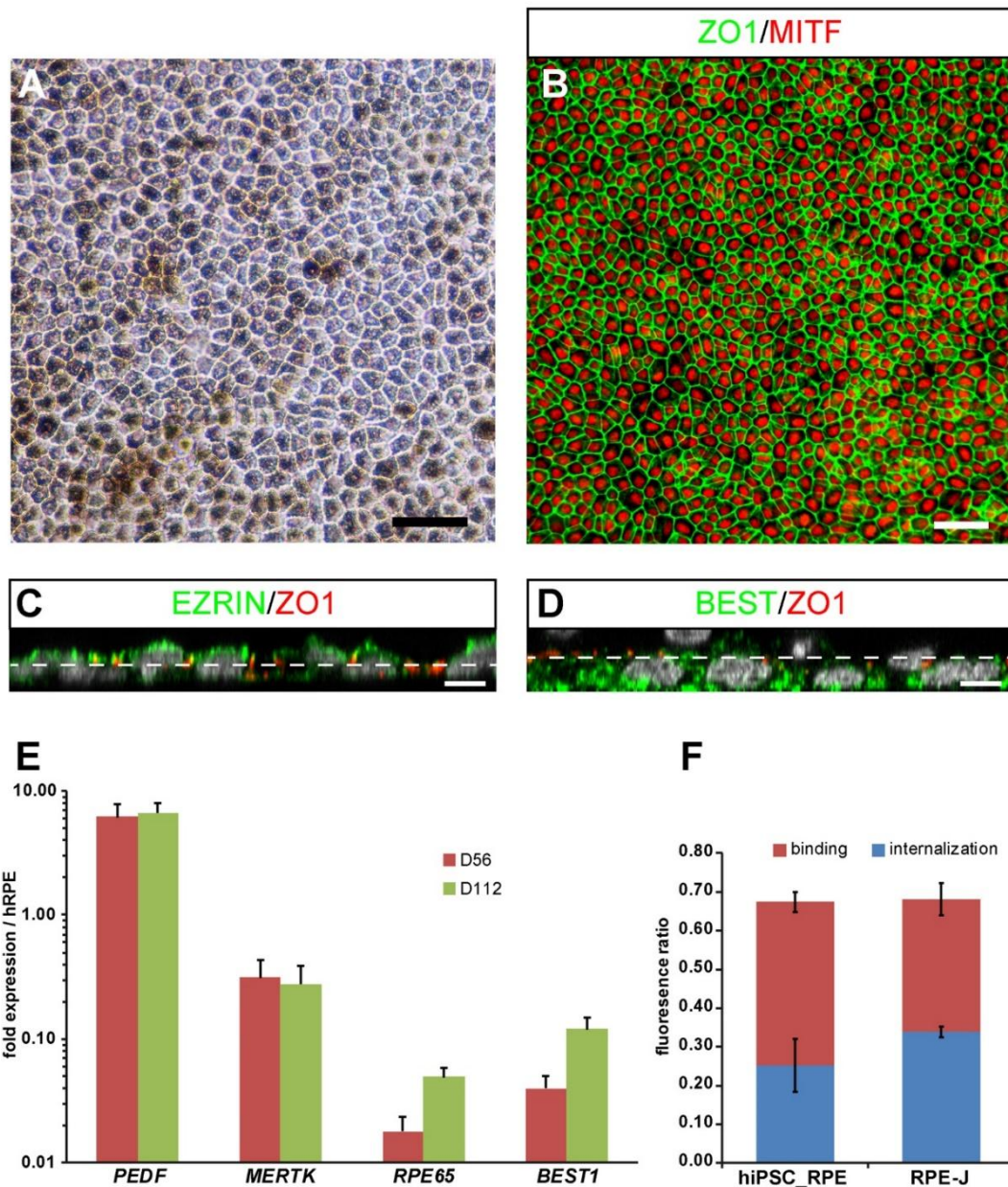


Figure 6: Generation of RPE cells from human MGC-derived iPSCs

(A) Phase-contrast images of RPE cells derived from iPSC-5f at passage 1 (P1), four weeks after picking. (B) ZO-1 and MITF immunostaining of hiPSC-derived RPE cell monolayer four weeks after picking. (C, D) XZ views after orthogonal reconstruction of confocal stacks showing typical polarized expression of BEST1 (basal) and Ezrin (apical), four weeks after picking. Dash line mark out the apical and basolateral compartments according to ZO1 labeling. (E) qRT-PCR analysis of mature RPE markers in human iPSC-derived RPE cells at P1, and P2. Data are normalized to control RNA isolated from human adult RPE cells. (F) Evaluation of ratio of FITC/DAPI fluorescence in human iPSC-derived RPE cells at P1 and in control RPE-J cell line after 3 h incubation with FITC-labeled POS to determine RPE cell phagocytic activity; Binding and uptake of POS were assayed as described Materials and Methods. (Scale bars: A, B, 50µm; C, D, 5µm).